



## Glacial geomorphology of the Kola Peninsula and Russian Lapland

Benjamin M. Boyes, Danni M. Pearce & Lorna D. Linch

To cite this article: Benjamin M. Boyes, Danni M. Pearce & Lorna D. Linch (2021) Glacial geomorphology of the Kola Peninsula and Russian Lapland, Journal of Maps, 17:2, 485-503, DOI: [10.1080/17445647.2021.1970036](https://doi.org/10.1080/17445647.2021.1970036)

To link to this article: <https://doi.org/10.1080/17445647.2021.1970036>



© 2021 The Author(s). Published by Informa UK Limited, trading as Taylor & Francis Group on behalf of Journal of Maps



[View supplementary material](#)



Published online: 06 Sep 2021.



[Submit your article to this journal](#)



Article views: 576



[View related articles](#)



[View Crossmark data](#)



## Glacial geomorphology of the Kola Peninsula and Russian Lapland

Benjamin M. Boyes<sup>a</sup>, Danni M. Pearce<sup>b</sup> and Lorna D. Linch<sup>a</sup>

<sup>a</sup>School of Environment and Technology, University of Brighton, Brighton, UK; <sup>b</sup>Faculty of Environmental Science and Natural Resource Management, Norwegian University of Life Sciences, Postbox 5003, 1433, Ås, Norway

### ABSTRACT

At present, there remains uncertainty surrounding the glacial history of the Fennoscandian Ice Sheet on the Kola Peninsula and Russian Lapland, northwest Arctic Russia. This is attributed to the lack of high-resolution ice sheet-scale geomorphological data in the region. This paper presents 245,997 landforms in a new high-resolution, glacial geomorphological map of the Kola Peninsula and Russian Lapland. Individual landforms were mapped from relief-shaded renditions of the 2 m resolution ArcticDEM alongside 3 m resolution PlanetScope Ortho Scene data in a Geographic Information System (GIS). Digital mapping was accompanied by field mapping in selected areas. The map, which is presented at a scale of 1: 675,000, will form the basis of a palaeoglaciological reconstruction of northwest Arctic Russia that will inform ice sheet dynamics – at both a regional- and ice sheet-scale – and provide an important framework through which numerical ice sheet models can be constrained.

### ARTICLE HISTORY

Received 10 February 2021  
Revised 23 July 2021  
Accepted 1 August 2021

### KEYWORDS

Glacial geomorphology;  
Fennoscandian Ice Sheet;  
Kola Peninsula; Russian  
Lapland; Arctic Russia

### 1. Introduction

The Kola Peninsula and Russian Lapland, northwest Arctic Russia (Figure 1), is a glaciologically significant region that was at the confluence of three dynamically different ice masses during the Late Weichselian (*c.* 40–10 ka): (i) the continental Fennoscandian Ice Sheet (FIS), which nucleated to the west of the Kola Peninsula and Russian Lapland; (ii) the White Sea Ice Stream (which drained the northeastern sector of the FIS) flowing along the southern Kola Peninsula coastline; and (iii) the marine Barents Sea Ice Sheet, which glaciated the area to the north of the Kola Peninsula and Russian Lapland (Hättestrand & Clark, 2006a; Hughes et al., 2016; Stroeven et al., 2016; Svendsen et al., 2004; Yevzerov, 2015).

Despite several attempts to reconstruct the glacial history (e.g. Boyes et al., 2021; Ekman & Iljin, 1991; Hättestrand & Clark, 2006b; Hughes et al., 2016; Lavrova, 1960; Niemelä et al., 1993; Stroeven et al., 2016; Svendsen et al., 2004), ice dynamics on the Kola Peninsula and neighbouring Russian Lapland remain poorly understood. Geomorphological evidence of the build-up of the FIS in the region is limited, and existing evidence of ice sheet advance across the region is often restricted to a disparate sedimentary record (Boyes et al., 2021; Hughes et al., 2016; Stroeven et al., 2016). Consequently, geomorphological interpretations of northwest Arctic Russia are inconsistent, resulting in four conflicting models of

glaciation during the Last Glacial-Interglacial Transition (LGIT; *c.* 20–10 ka): (i) initial rapid deglaciation of the FIS on the eastern Kola Peninsula, with ice lobes occupying the surrounding lowlands and straits (Niemelä et al., 1993); (ii) coherent FIS retreat, inland from the coasts (Hättestrand & Clark, 2006b); (iii) the existence of a dynamically independent Ponoy Ice Cap on the Kola Peninsula (Rainio et al., 1995); and (iv) rapid retreat of the FIS, followed by subsequent glaciation by the Kara Sea Ice Sheet from the northeast (Grosswald & Hughes, 2002). Furthermore, different Younger Dryas (*c.* 12.8–11.7 ka) ice-marginal zone geometries exist for each of these four LGIT scenarios (Boyes et al., 2021). The Kola Peninsula and Russian Lapland is, therefore, a major sector of the FIS where glaciation is poorly understood (Hughes et al., 2010; Stroeven et al., 2016).

Recent advances in our understanding of palaeo-ice sheet signatures and ice dynamics (e.g. Chandler et al., 2018; Chiverrell et al., 2020; Clark et al., 2018; Hughes et al., 2016; Lewington et al., 2020; McMartin et al., 2021; Peterson et al., 2017; Stokes et al., 2015; Stokes et al., 2016; Stroeven et al., 2016), coupled with the availability of new high-resolution digital elevation models (DEM) and satellite imagery, warrants a fresh investigation into Late Weichselian glaciation of northwest Arctic Russia. We present a new high-resolution glacial geomorphological dataset of glacial landforms and sediments from the Kola Peninsula

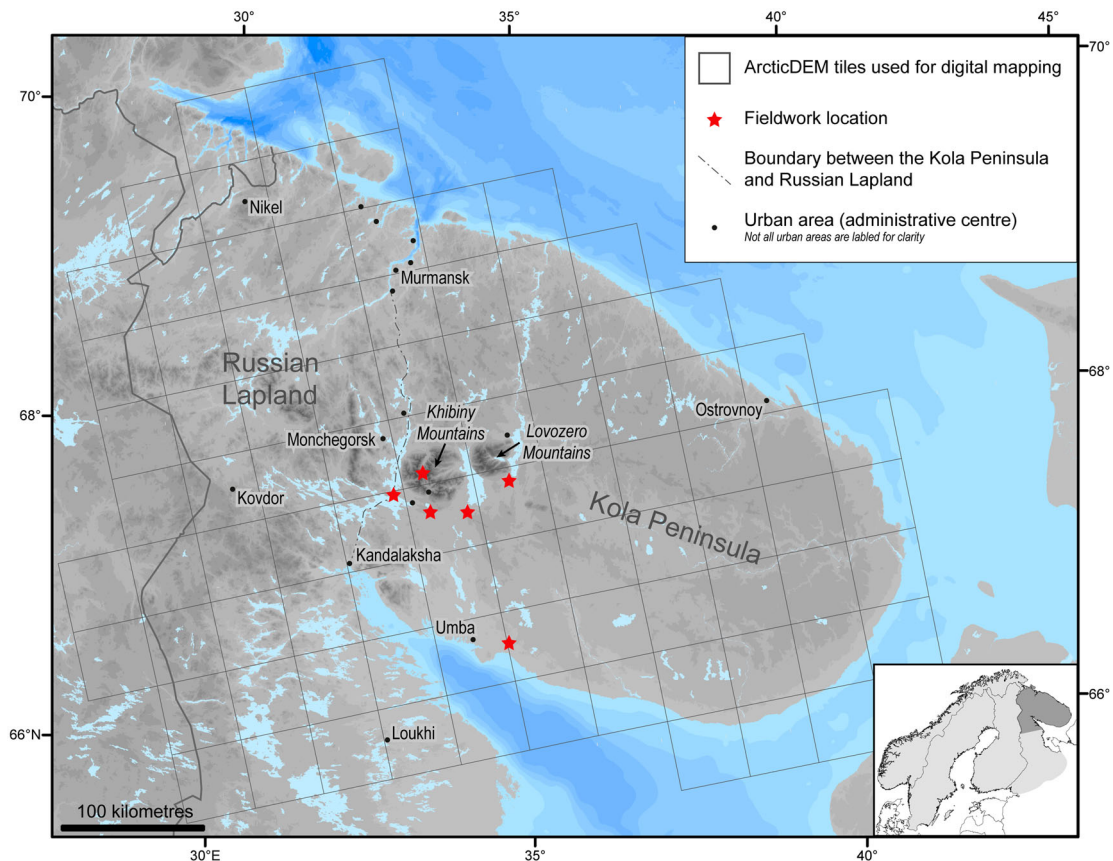


**Figure 1.** The Kola Peninsula and Russian Lapland, northwest Arctic Russia, including areas visited during fieldwork. The ArcticDEM tiles used during the digital mapping stage are shown; PlanetScope Ortho Scene data (not shown) covers the mapped area. The map extends at least 5 km over the Russian border into Norway and Finland, and the southern extent of mapping between the Russian-Finnish border and the White Sea coastline is defined by the selected ArcticDEM tiles. Topography and bathymetry data in this figure are from the European Space Agency (2021), [GEBCO Compilation Group \(2020\)](#) GEBCO 2020 Grid. Topography is shaded dark-light grey with darker shades representing higher ground and bathymetry is shaded dark-light blue with darker shades representing greater depth; for a detailed legend refer to the Main Map. Inset: the Fennoscandian shield shaded light grey and the mapped area shaded dark grey.

and Russian Lapland. This dataset will permit the development of a new glacial reconstruction of northwest Arctic Russia, which will inform ice sheet dynamics – at both a regional- and ice sheet-scale – and provide an important framework through which numerical ice sheet models can be constrained.

## 2. Methods

The methods used in the production of this glacial geomorphological map are based on [Smith and Clark \(2005\)](#), [Greenwood and Clark \(2008\)](#), [Hughes et al. \(2010\)](#), and [Chandler et al. \(2018\)](#), among others, all of whom have successfully demonstrated the use of remotely sensed imagery for mapping palaeo-glacial landscapes. The Main Map covers >164,700 km<sup>2</sup> of northwest Arctic Russia and represents over 1500 hours of work conducted over a period of 18 months.

### 2.1. Datasets and data processing

The Main Map has been produced at a scale of 1:675,000 based on two forms of high-resolution

remotely sensed imagery: (i) the ArcticDEM Digital Surface Model (DSM), and (ii) PlanetScope Ortho Scene data ([Figure 2](#)). The ArcticDEM, which has a spatial resolution of 2 m (vertical accuracy of 2 m and horizontal accuracy of 3.8 m), was converted into hillshaded relief models for meaningful graphical and analytical purposes. To avoid azimuth bias, four hillshaded relief images were generated for the entire region: two images with the sun placed at orthogonal angles of 45° (NE) and 315° (NW) generated with an illumination angle of 30°, a third image with an illumination angle of 90° (i.e. ‘overhead’), and a fourth multidirectional hillshade image that combines light sources from six different directions ([Figure 2](#)). All images were vertically exaggerated by three times to enhance subtle features. PlanetScope Ortho Scene data are orthorectified, georeferenced daily satellite images with a ground sample distance of 3.7 m. Individual scenes with the least atmospheric obstructions (i.e. clouds, dust, and thick snow cover) were chosen and combined into a single seamless image, which was viewed in full-colour composite and near-infrared ([Figure 2](#)).

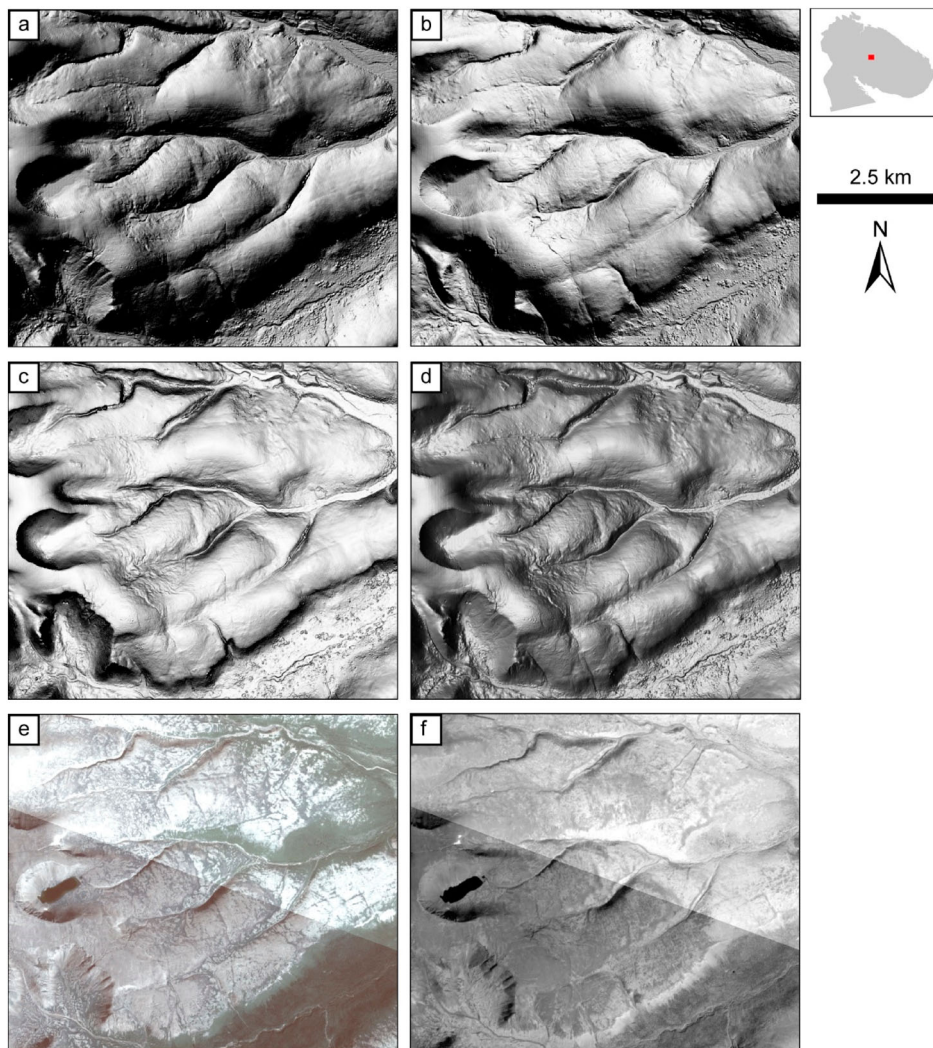


**Figure 2.** Examples of the imagery used during the digital mapping stage from the Khibiny Mountains showing the resolution of data sources as well as different images derived from each data source. Four hillshaded relief images were derived from the 2 m resolution ArcticDEM: (a) azimuth 315°, illumination angle 30°; (b) azimuth 45°, illumination angle 30°; (c) illumination angle 0° (i.e. overhead); and (d) multidirectional (which combines light sources from six different directions as opposed to a single direction). All hillshaded relief models were vertically exaggerated three times to enhance subtle landforms. PlanetScope Ortho Scene data with 3 m resolution were displayed in (e) full colour and (f) near-infrared. Near-infrared imagery allowed snow patches and water bodies to be easily observed and thus excluded from the map.

## 2.2. Mapping procedure

*Google Earth Pro* was used for 3D landform visualisation and virtual reconnaissance prior to digital mapping and fieldwork. Digital mapping was achieved through visual identification and onscreen vectorisation of individual landforms (discussed in Section 3) within a Geographic Information System (GIS) environment. Visual identification of glacial landforms was an integrated process involving several consultations of the DEM and satellite imagery. Repeated passes of the mapped area were made at a range of scales to ensure that features of all sizes were discernible on the imagery. Mapping style (i.e. polyline or polygon) for each landform type considers the most appropriate representation of landform size, orientation, and shape (Tables 1 and 2). Polylines map

the crest-line of individual landforms while polygons map the break-of-slope outline of individual landforms. The diagnostic criteria used to identify landforms are outlined in Table 2.

Remote digital mapping was also accompanied by five weeks of field mapping in 2019. Extensive fieldwork was not possible in this remote region, thus field mapping primarily aimed to verify the digital mapping process. Fieldwork was undertaken in and around the accessible areas of Apatity, Kirovsk, Monchegorsk, and Umba (Figure 1).

The Main Map was produced in *ESRI® ArcMap™ 10.7.1*. Individual vectors were smoothed for cartographic purposes, although caution was taken to ensure the morphologies of the mapped landforms were not lost. Mapped landforms were subsequently classified, where applicable, into different categories

**Table 1.** Mapped landforms, mapping style, their occurrence, and estimated completeness.

Mapped landform	Mapping style	Occurrence		Completeness (%)
		<i>By confidence level</i>		
<b>Subglacial bedforms</b>				
Subglacial lineations	Polyline	Total:	58,113	90
		High (3):	50,503	
		Medium (2):	6516	
		Low (1):	1094	
Subglacial ribs	Polygon	Total:	8293	90
		High (3):	6446	
		Medium (2):	1594	
		Low (1):	253	
Subglacially streamlined bedrock	Polyline	Total:	1969	80
		High (3):	971	
		Medium (2):	895	
		Low (1):	103	
<b>Meltwater landforms</b>				
Meltwater channels	Polyline	Total:	96,040	80
		High (3):	60,449	
		Medium (2):	35,399	
		Low (1):	192	
Eskers	Polyline	Total:	3358	90
		High (3):	2240	
		Medium (2):	809	
		Low (1):	309	
Palaeo-lake shorelines	Polyline	Total:	208	50
		High (3):	29	
		Medium (2):	105	
		Low (1):	74	
Glaciofluvial deposits	Polygon	Total:	1409	75
		High (3):	1042	
		Medium (2):	325	
		Low (1):	42	
<b>Morainic landforms</b>				
Moraine ridges	Polyline	Total:	3967	85
		High (3):	1886	
		Medium (2):	1641	
		Low (1):	440	
Moraine deposits	Polygon	Total:	72,191	85
		High (3):	52,086	
		Medium (2):	17,259	
		Low (1):	2846	
Cirque infills <sup>a</sup>	Polygon	Total:	40	95
		High (3):	22	
		Medium (2):	16	
		Low (1):	2	
Cirque infill hummocks	Polygon	Total:	163	95
		High (3):	158	
		Medium (2):	5	
		Low (1):	–	
Cirque infill ridges	Polyline	Total:	54	95
		High (3):	46	
		Medium (2):	8	
		Low (1):	–	
<b>Cirques</b>				
Cirques <sup>b</sup>	Polyline	Total:	192	100
		Grade 1:	28	
		Grade 2:	33	
		Grade 3:	29	
		Grade 4:	23	
		Grade 5:	79	
<b>Total number of mapped landforms</b>			245,997	

<sup>a</sup>Cirque infill surface features are mapped as polygons (hummocks;  $n = 163$ ) and polylines (ridges;  $n = 54$ ), and are granted the same level of confidence as their parent cirque infill deposit.

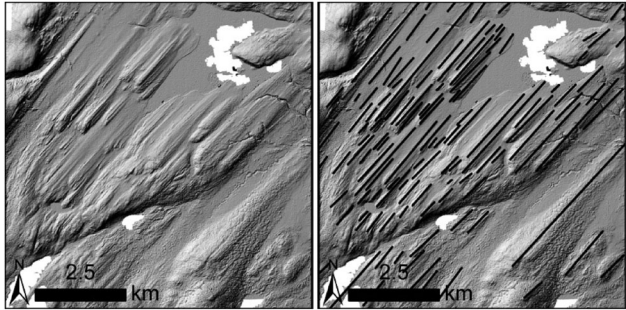
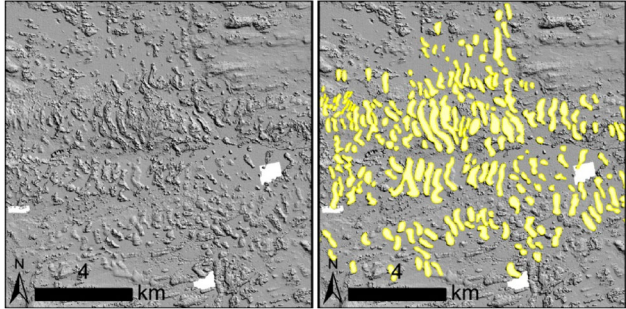
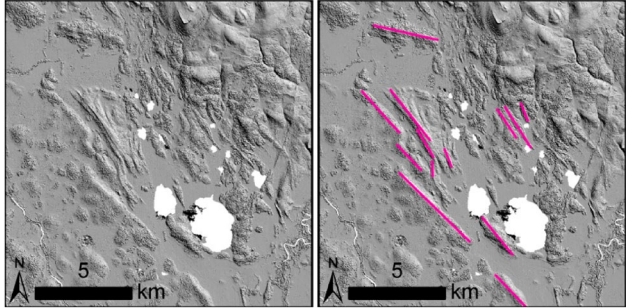
<sup>b</sup>Confidence levels are not applied to cirques since cirque grades already imply a subjective level of confidence (Evans & Cox, 1995).

in the attribute table of each shapefile to support interpretations of ice dynamics (see Table 2 for the landform classifications and diagnostic criteria of landforms identified in northwest Arctic Russia). Applying landform classifications is a useful and undemanding additional step when following clearly defined diagnostic criteria such as those outlined in Table 2, and is necessary for glacial interpretations beyond, for example, simple ice flow patterns or ice

margin positions. Individual landforms also are attributed a subjective level of confidence so that future glacial reconstructions are developed with the greatest certainty by excluding lower confidence landforms. The confidence levels are based on the following criteria:

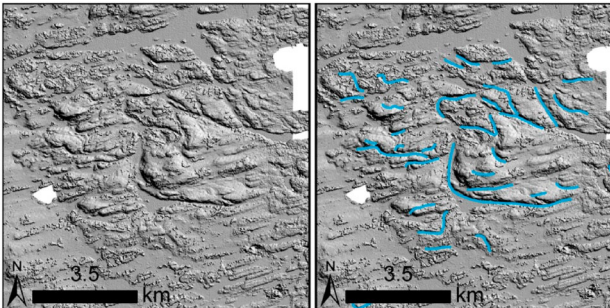
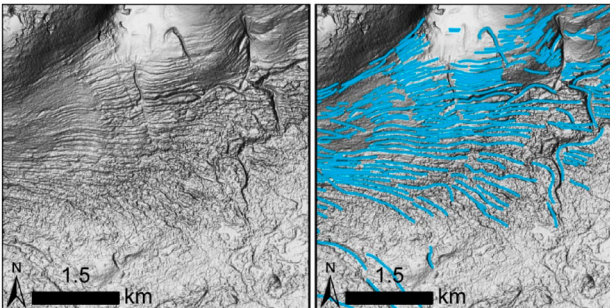
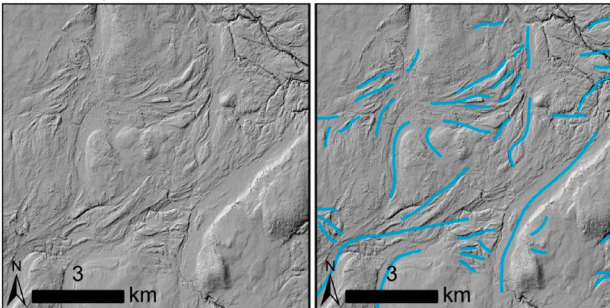
*Low confidence (1):* landform may not be of glacial origin, landform may be misinterpreted, and the boundaries of the mapped landform are likely inaccurate.

**Table 2.** Diagnostic criteria used to identify glacial landforms in the Kola Peninsula and Russian Lapland, northwest Arctic Russia, for the purpose of compiling the Main Map. Landform types were selected on the basis of (i) landforms identified during the reconnaissance mapping stage, and (ii) the requirements of the glacial inversion model (see Kleman and Borgström, 1996) that will be used in a future publication to reconstruct the pattern of glaciation in northwest Arctic Russia. To aid interpretations of ice dynamics during the glacial reconstruction some landforms have been classified according to the morphologies identified in northwest Arctic Russia. For the numbers of mapped landforms see Table 1. Annotated figures of the ArcticDEM imagery accompany each landform type: the symbology used matches the Main Map. Data gaps in the ArcticDEM imagery are represented by white spaces. DEM courtesy of the Polar Geospatial Center (Porter et al., 2018). These criteria can also be used as a resource when mapping other formerly glaciated landscapes.

Landform (Classification, where applicable)	Diagnostic criteria (Based on the criteria of ...)	Example (left: ArcticDEM imagery) (right: annotated ArcticDEM imagery)
<b>Subglacial lineations</b>	Based on the criteria of <i>Greenwood and Clark (2008), Bennett and Glasser (2009), and Hughes et al. (2010)</i> <ul style="list-style-type: none"> <li>• Streamlined landforms aligned parallel to the ice flow direction</li> <li>• Elongated ellipse in planform, with steep stoss slopes and gentle lee slopes in profile</li> <li>• Typically found in swarms</li> <li>• Flutings: heights &lt;5 m, widths &lt;5 m, lengths 10–&gt;100 m</li> <li>• Drumlins, crag and tails: heights 5–50 m, lengths 10–3000 m</li> <li>• Mega-scale glacial lineations (MSGL): lengths 8–70 km, widths 200–1300 m</li> </ul>	 <p data-bbox="1473 699 1682 719">68°59'58"N, 30°59'32"E</p>
<b>Subglacial ribs</b>	Based on the criteria of <i>Greenwood and Clark (2008), Bennett and Glasser (2009), and Hughes et al. (2010)</i> <ul style="list-style-type: none"> <li>• Tabular or ripple-like ridges that are transverse to the ice flow direction</li> <li>• Sizes ranging from metres to kilometres in length</li> <li>• Occur in 'fields'</li> <li>• Transition into, or associated with, lineations</li> </ul>	
<b>Subglacially streamlined bedrock</b>	Based on the criteria of <i>Bennett and Glasser (2009), Benn and Evans (2010), and Clark et al. (2018)</i> <ul style="list-style-type: none"> <li>• Streamlined bedrock surfaces, similar in appearance to subglacial lineations</li> <li>• May be geologically controlled, or may be mistaken for geological faults</li> <li>• Roches moutonnées – asymmetric bedrock bumps with abraded stoss faces and quarried lee faces; widths &lt;1 m to 100s m</li> <li>• Whalebacks – symmetrical bedrock bumps with abraded stoss and lee slopes; widths &gt;100 m</li> </ul>	 <p data-bbox="1473 1415 1682 1436">67°28'40"N, 36°45'48"E</p>

(Continued)

**Table 2.** Continued.

<b>Landform</b> (Classification, where applicable)	<b>Diagnostic criteria</b> (Based on the criteria of ...)	<b>Example</b> (left: ArcticDEM imagery) (right: annotated ArcticDEM imagery)
<b>Meltwater channels</b> <i>Subglacial</i>	<p data-bbox="414 264 1084 287"><i>Based on the criteria of Greenwood et al. (2007) and Bennett and Glasser (2009)</i></p> <ul data-bbox="414 292 1084 600" style="list-style-type: none"> <li>• Undulating long profiles</li> <li>• Descent downslope may be oblique</li> <li>• Steep descent downslope may occur</li> <li>• Complex systems – bifurcating and anastomosing</li> <li>• High sinuosity</li> <li>• Abandoned loops</li> <li>• Abrupt beginnings and ends</li> <li>• Absence of glaciofluvial deltas (diagnostic criteria below)</li> <li>• Cavity systems and potholes</li> <li>• Ungraded confluences</li> <li>• Variety of sizes and forms within the same connected system</li> <li>• Can be associated with eskers (diagnostic criteria below)</li> <li>• May be occupied by contemporary fluvial drainage networks</li> </ul>	
<i>Lateral</i>	<ul data-bbox="414 660 1234 826" style="list-style-type: none"> <li>• Perched on valley sides, where they may be subparallel or diagonal to contemporary contours</li> <li>• May form a 'stack' of channels on a valley side subparallel to each other</li> <li>• Approximately straight channels, often for long distances</li> <li>• May terminate in downslope chutes (steep channel conveying channels to a lower elevation)</li> <li>• May terminate abruptly</li> <li>• May be found in isolation from other glacial landforms</li> <li>• May be occupied by contemporary fluvial drainage networks</li> </ul>	
<i>Proglacial</i>	<ul data-bbox="414 1031 1043 1171" style="list-style-type: none"> <li>• Regular meander bends</li> <li>• May form networks with occasional bifurcation</li> <li>• Flow directly downslope</li> <li>• Large dimensions – channels may be wide and deep</li> <li>• May be occupied by contemporary fluvial drainage networks</li> <li>• May be associated with glaciofluvial deposits (diagnostic criteria below)</li> </ul>	

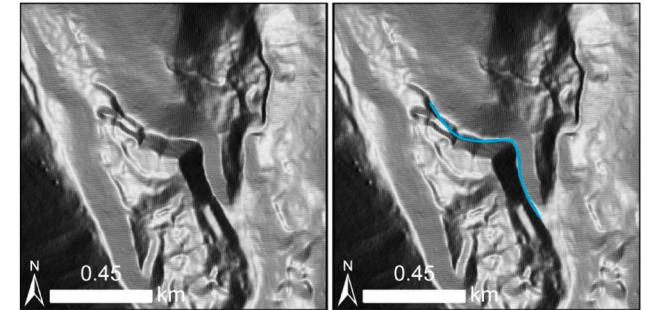
66°17'45"N, 32°37'25"E

67°43'44"N, 34°48'51"E

66°28'26"N, 40°28'20"E

### Spillway

- Abrupt beginnings, usually at palaeo-lake shorelines (diagnostic criteria below)
- May terminate abruptly
- May be found in isolation (of other meltwater channels)
- Associated with ice-dammed lakes (see palaeo-lake shorelines, below)
- Channel may incise moraine deposits or glaciofluvial deposits
- Channel direction may be controlled by the surrounding topography

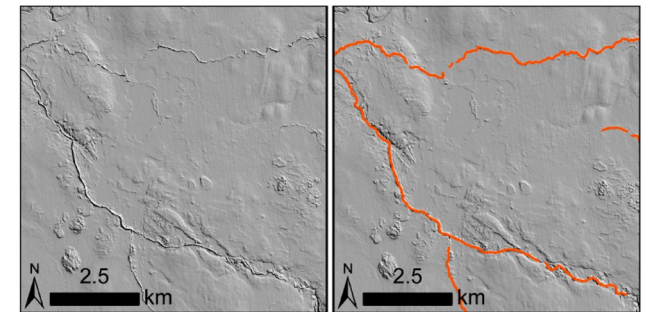


67°41'41"N, 33°38'40"E

### Eskers

Based on the criteria of [Storrar et al. \(2014\)](#)

- Elongate, sinuous ridges, or may be segmented or beaded
- Can be single ridges or complex braided systems
- Aligned subparallel to subglacial lineations (diagnostic criteria above) and ice flow direction



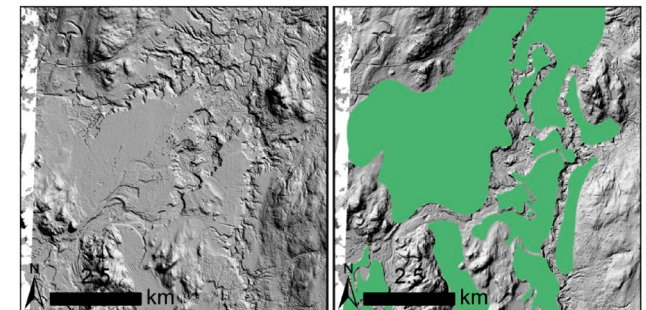
66°41'00"N, 40°12'54"E

### Glaciofluvial deposits

Based on the criteria of [Bennett et al. \(2000\)](#), [Hättestrand and Clark \(2006a\)](#), [Bennett and Glasser \(2009\)](#), and [Evans and Orton \(2015\)](#)

#### Outwash

- Areas with relatively flat upper surfaces, may have kame and kettle topography on surfaces
- May have a braided meltwater channel system atop of deposits (diagnostic criteria above)
- May be associated with eskers (diagnostic criteria above)
- May have distinct colouring compared to the surrounding landscape (e.g. yellow-brown sandy colour)

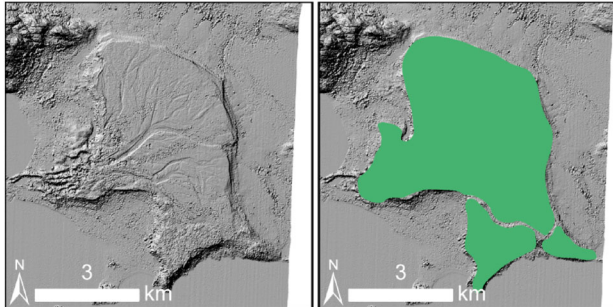
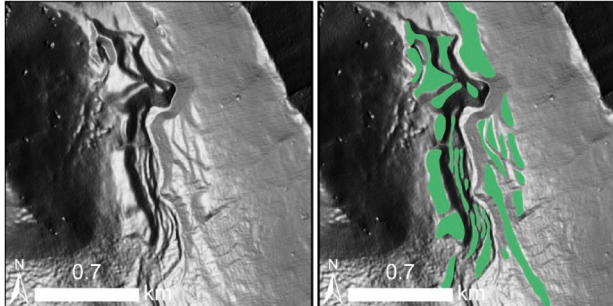
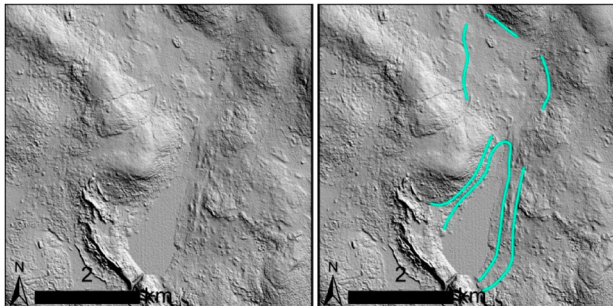


69°23'59"N, 30°59'00"E

(Continued)



**Table 2.** Continued.

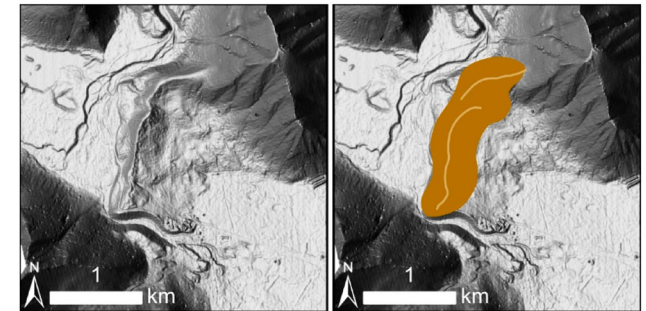
Landform (Classification, where applicable)	Diagnostic criteria (Based on the criteria of ...)	Example (left: ArcticDEM imagery) (right: annotated ArcticDEM imagery)
Delta	<ul style="list-style-type: none"> <li>• Fan-shaped outwash deposits with apex up-ice; apices may be associated with eskers (diagnostic criteria above)</li> <li>• Areas with relatively flat upper surfaces, may have kame and kettle topography on surfaces</li> <li>• May have braided river system atop of fans</li> <li>• May have distinct colouring compared to the surrounding landscape (e.g. yellow-brown sandy colour)</li> </ul>	 <p data-bbox="1473 576 1684 600">66°17'39"N, 30°57'42"E</p>
Terrace	<ul style="list-style-type: none"> <li>• Outwash sediments banked on valley sides with relatively flat upper surfaces and steep sides</li> <li>• May have a contemporary river system dissecting the terraces</li> <li>• May have distinct colouring compared to the surrounding landscape (e.g. yellow-brown sandy colour)</li> <li>• May be associated with palaeo-lake shorelines (diagnostic criteria below)</li> <li>• May be associated with De Geer moraines (diagnostic criteria below)</li> </ul>	 <p data-bbox="1473 946 1684 970">67°41'37"N, 33°35'40"E</p>
Palaeo-lake shorelines	<p data-bbox="416 1010 831 1029"><i>Based on the criteria of Bennett and Glasser (2009)</i></p> <ul style="list-style-type: none"> <li>• Horizontal benches with a faint terrace-like form on hillsides</li> <li>• May be found in association with terrace outwash deposits and/or delta deposits (diagnostic criteria above)</li> <li>• May be associated with moraine deposits (diagnostic criteria below)</li> </ul>	 <p data-bbox="1473 1316 1684 1340">68°24'55"N, 34°31'31"E</p>

**Moraine deposits/ridges**

Based on the criteria of Hättestrand and Clark (2006a), Smith et al. (2006), Bennett and Glasser (2009), Evans et al. (2014), Peterson et al. (2017) and Ojala et al. (2021)

*End*

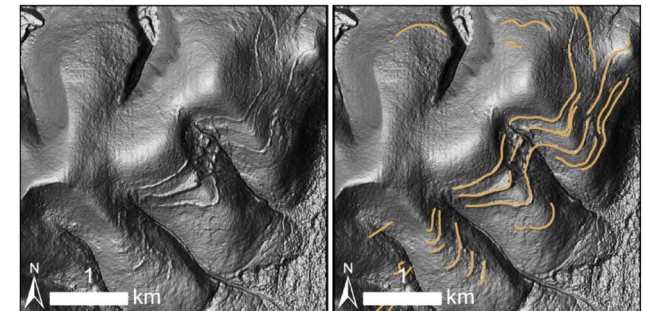
- Ridges perpendicular to the ice flow direction
- May be breached by channel features
- May be arcuate
- Heights vary from a few metres to several 10s metres
- Tendency for steeper lee slopes compared to stoss slopes
- Stoss slopes may display evidence of glacial modification



67°39'51"N, 33°39'17"E

*Lateral*

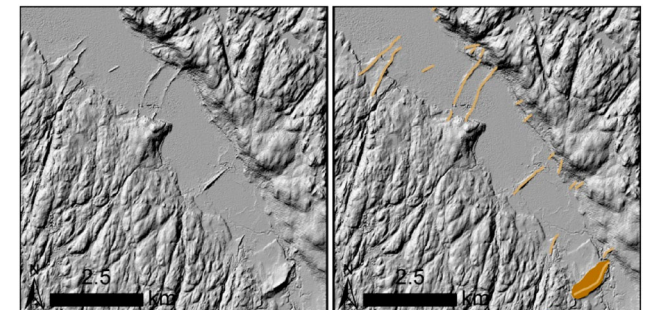
- Ridges parallel to the ice flow direction
- May be modified by meltwater channels and post-glacial modification
- Outwash terraces may be superimposed upon proximal slopes
- Cross-valley asymmetry, one valley side larger than the other



67°36'59"N, 34°04'56"E

*De Geer*

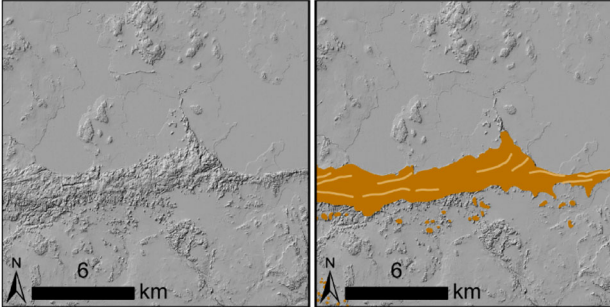
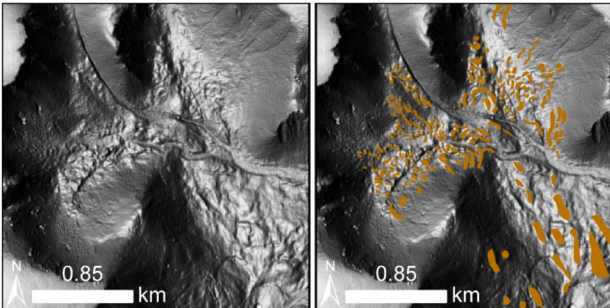
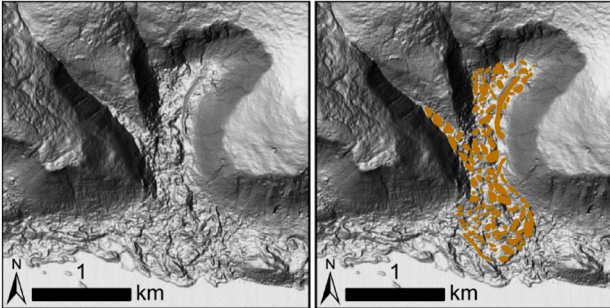
- Ridges across a valley floor, perpendicular to the ice flow direction
- Straight or slightly concave in planform
- Low heights <5 m
- Associated with palaeo-shorelines (marine and lake), where the ridges abruptly start and end



68°15'25"N, 38°45'36"E

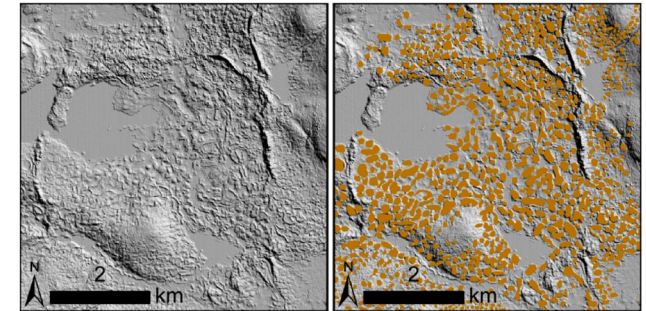
(Continued)

Table 2. Continued.

Landform (Classification, where applicable)	Diagnostic criteria (Based on the criteria of ...)	Example (left: ArcticDEM imagery) (right: annotated ArcticDEM imagery)
<i>Interlobate</i>	<ul style="list-style-type: none"> <li>• Large ridges and hummocky deposits</li> <li>• Ridges display tabular morphologies with relatively flat upper surfaces and steep slopes on either side of the moraines</li> <li>• May have kettle topography on the flat upper surfaces</li> <li>• May have lateral meltwater channels on the upper surfaces subparallel to ridge crests/moraine sides</li> <li>• May be surrounded by smaller hummocky topography</li> <li>• Associated with glaciofluvial deposits and eskers, which can appear to 'feed' both sides of the moraine</li> </ul>	 <p data-bbox="1476 596 1682 619">66°20'43"N, 38°05'59"E</p>
<i>Hummock – Type 1a</i>	<ul style="list-style-type: none"> <li>• Small irregular mounds interspaced with depressions in mountainous environments</li> <li>• Occur in large spreads</li> <li>• Orientations indicate ice flowing up-valley/retreating down-valley</li> </ul>	 <p data-bbox="1476 963 1682 986">67°43'16"N, 33°42'55"E</p>
<i>Hummock – Type 1b</i>	<ul style="list-style-type: none"> <li>• Small irregular mounds and depressions in mountainous environments</li> <li>• Generally occur in large spreads</li> <li>• Orientations indicate ice flowing down-valley/retreating up-valley</li> </ul>	 <p data-bbox="1476 1335 1682 1358">67°50'00"N, 34°50'29"E</p>

*Hummock – Type 2a*

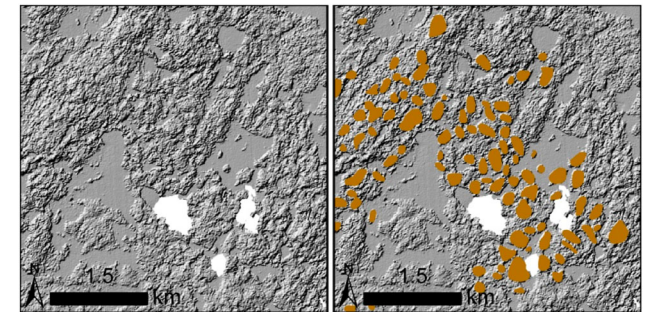
- Ring-shaped deposits, with depressions in the centre
- Rings vary in size: 1–>30 m in diameter
- May have irregular ridges in all directions in addition to rings
- May have small irregular mounds in addition to rings and ridges
- Often occur in large spreads



68°06'03"N, 34°00'46"E

*Hummock – Type 2b*

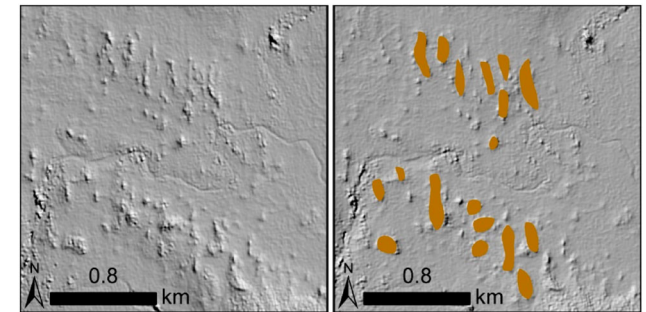
- Small irregular mounds and depressions
- Generally occur in large spreads
- Disorganised distribution



66°27'20"N, 35°39'55"E

*Hummock – Type 2c*

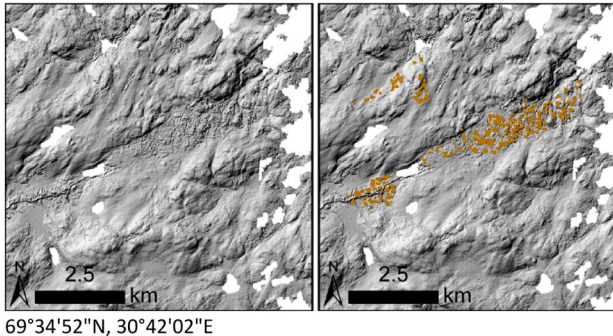
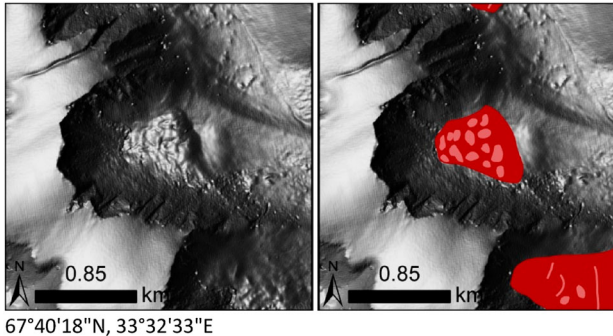
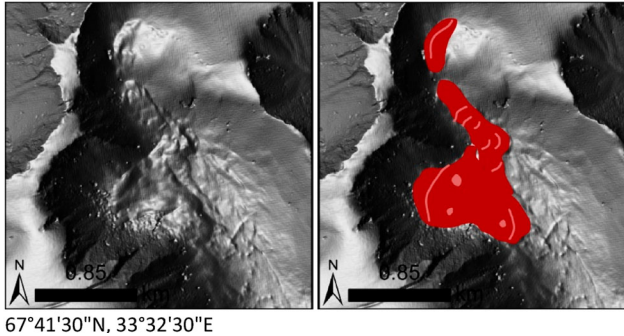
- Tabular or ripple-like ridges transverse to ice flow direction – morphologically similar to subglacial ribs, but smaller
- Semi-ordered, irregular collections of ridges and mounds
- Not found in association with subglacial bedforms



67°25'38"N, 35°30'34"E

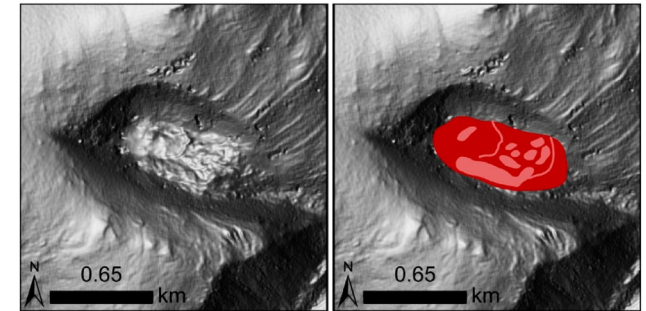
(Continued)

**Table 2.** Continued.

Landform (Classification, where applicable)	Diagnostic criteria (Based on the criteria of ...)	Example (left: ArcticDEM imagery) (right: annotated ArcticDEM imagery)
Hummock – Type 3	<ul style="list-style-type: none"> <li>• Hummocks associated with sub-glacial drainage</li> <li>• May be small irregular mounds and depressions</li> <li>• Hummock morphology may be V-shaped with apices pointed down-ice as well as gentle up-ice and steep down-ice slopes</li> <li>• May appear in tracts parallel to ice flow</li> <li>• Tracts may be perpendicular to ice margin positions (indicated by morainic deposits)</li> <li>• Tracts may be topographically controlled</li> <li>• May be associated with eskers and/or subglacial meltwater channels (diagnostic criteria above)</li> </ul>	 <p>69°34'52"N, 30°42'02"E</p>
Cirque infills <sup>a</sup> Type 1	<p><i>Based on the criteria of Hättestrand et al. (2008) and Sugden and Hall (2020)</i></p> <ul style="list-style-type: none"> <li>• Morainic deposits located on cirque floors: typically banked against cirque headwalls, and spread across cirque floors</li> <li>• May have convex up-valley (against cirque headwalls) slopes</li> <li>• Terrace-like deposits with steep, concave down-valley slopes</li> <li>• Irregular hummocky surfaces</li> </ul>	 <p>67°40'18"N, 33°32'33"E</p>
Type 2	<ul style="list-style-type: none"> <li>• Morainic deposits located on cirque floors: typically banked against cirque headwalls, and spread across cirque floors</li> <li>• May have a convex up-valley (against cirque headwalls) slopes</li> <li>• Deposits with down-valley slopes extend out towards the main valley</li> <li>• May have flow deformation structures on the surface such as irregular ridges and hummocks</li> </ul>	 <p>67°41'30"N, 33°32'30"E</p>

Type 3

- Morainic deposits located on cirque floors: typically banked against cirque headwalls, and spread across cirque floors
- Slightly convex profiles
- Smooth undulating surfaces that may be fluted
- May have surface ridges and hummocks resembling end moraines
- Typically have a semi-circular ring of lakes along cirque headwalls

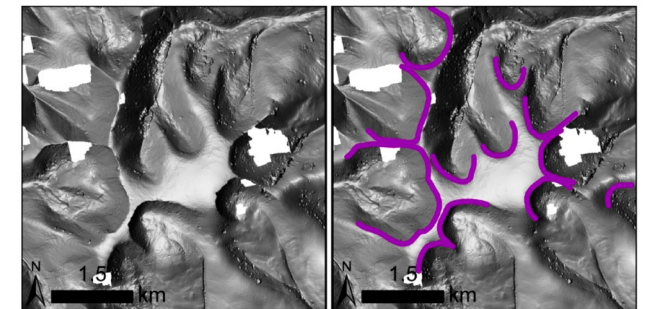


67°50'20"N, 34°59'00"E

Cirques

Based on the criteria of [Evans and Cox \(1995\)](#), [Benn and Evans \(2010\)](#), and [Barr and Spagnolo \(2015\)](#)

- Amphitheatre-shaped hollows, open down-valley with steep headwalls
- Arcuate shape of headwalls (in both planform and profile)
- Gently sloping floors, often occupied by a lake, bog, or cirque infill
- *Cirque development is classified after [Evans and Cox \(1995\)](#): Grade 1 'classic cirque'; Grade 2 'well-defined'; Grade 3 'definite'; Grade 4 'poor'; Grade 5 'marginal cirque'*
- *Cirque types are defined after [Benn and Evans \(2010\)](#): Simple; Compound; Complex; Staircase; Trough*



67°50'00"N, 33°50'15"E

**Landform**

(Classification, where applicable)

**Diagnostic criteria**

(Based on the criteria of ...)

**Example**

(left: ArcticDEM imagery) (right: annotated ArcticDEM imagery)

<sup>a</sup>Surface features on cirque infills are mapped as either cirque infill hummocks or cirque infill ridges.

*Medium confidence (2)*: landform is likely of glacial origin, landform may be misinterpreted, and the boundaries of the mapped landform may be inaccurate.

*High confidence (3)*: landform is definitely of glacial origin, landform is correctly interpreted, and the boundaries of the mapped landform are accurate.

Elevation and bathymetry data for the base map are derived from the European Space Agency (2021) and the GEBCO Compilation Group (2020); this elevation data are for visualisation purposes only and were not used during the digital mapping stage. The map was exported to *Adobe Illustrator v24.2* for editing before being exported in PDF format. The final map is projected to the WGS1984 UTM Zone 36N system.

### 3. Mapped glacial landforms

The Main Map includes a total of 245,997 glacial landforms, which significantly extends the volume and detail of geomorphological data in the region. To allow scrutiny of individual landforms the map is designed to be printed at A0 size (1,189 by 841 mm). For clarity, the Main Map does not distinguish individual landform classifications; this data can be viewed in the shapefiles of the mapped landforms that are provided in the supplementary information and can be viewed in a GIS.

In this section, we discuss the mapped landforms. The occurrence and estimated completeness of mapped landforms can be found in Table 1. The diagnostic criteria of the landforms identified in the mapped region and examples of the mapped landforms in the ArcticDEM imagery are outlined in Table 2. It should be noted that Table 2 provides an overview of the principal diagnostic criteria of glacial landforms, but it is recognised that landform morphologies can vary. Furthermore, Table 2 is a resource to be used by others when mapping glaciated landscapes, not just for the purpose of understanding the Main Map. The confidence rating and (where applicable) classification applied to each individual landform can be viewed in the attribute table of the shapefiles provided in the supplementary information. No contemporary glaciers are identified on the Kola Peninsula and Russian Lapland. As such, all mapped landforms are from palaeo-glaciations. However, the Main Map does not address the ages of the mapped landforms and it is highly likely that not all landforms are derived from the Late Weichselian glaciation; the relative age of the mapped glacial landforms will be explored in future studies.

#### 3.1. Subglacial bedforms

Subglacial bedforms include **subglacial lineations** (glacially streamlined landforms formed parallel to

ice flow including, for example, drumlins, crag and tails, and mega-scale glacial lineations; Greenwood & Clark, 2008; Hughes et al., 2010), **subglacial ribs** (groups of regularly spaced ridges formed transverse to ice flow; Greenwood & Clark, 2008; Hughes et al., 2010), and **subglacially streamlined bedrock** (linear ridges of bedrock that are possibly related to the structural geology rather than to ice flow directions; Hughes et al., 2010). We use the term ‘subglacial ribs’ to (i) encapsulate all ribbed bedform types, such as ribbed moraines, Rogen moraines, and subglacial traction ribs, and (ii) because terminology that uses ‘moraines’ when describing subglacial ribs is misleading since, since it implies ice-marginal landforms rather than bedforms.

Subglacial lineations identified in northwest Arctic Russia show a large size range, from ~59 m to ~11 km in length, with a mean length of ~815 m. The longest lineations generally occur in areas where subglacial lineations have been mapped previously, such as the southwestern Kola Peninsula, and northern and southern Russian Lapland (Hättestrand & Clark, 2006a; Kleman et al., 1997; Niemelä et al., 1993). The map we present clearly reveals a paucity of subglacial bedforms on the central eastern Kola Peninsula. This contrasts with the western Kola Peninsula and Russian Lapland, where subglacial bedforms dominate the lowland terrain. This suggests diverse subglacial conditions during the Late Weichselian, including cold-based glaciation (indicated by a lack of subglacial bedforms in some areas) and warm-based glaciation (indicated by the presence of subglacial bedforms in other areas) (Hättestrand & Clark, 2006a; Kleman et al., 2008). Moreover, zones of densely-spaced subglacial lineations reveal ice stream pathways (corridors of fast-flowing ice bordered by slow-flowing ice; Stokes & Clark, 2001) on the western Kola Peninsula and Russian Lapland. There are 4,185 instances of bedform superimposition (i.e. where subglacial bedforms are observed overlapping other bedforms). Superimposition has been considered rarely in previous reconstructions (cf. Kleman et al., 1997; Winsborrow et al., 2010), whereas the mapped dataset, presented here, permits a multi-temporal record of ice flow patterns across northwest Arctic Russia.

#### 3.2. Meltwater landforms

Meltwater landforms include **meltwater channels** (relict channels that are the product of glacier ablation and meltwater flow; Greenwood et al., 2007), **eskers** (elongate, sinuous ridges composed of glaciofluvial sediments; Storrar et al., 2014), **glaciofluvial deposits** (accumulations of glaciofluvial material that mostly display planar upper surfaces; Bennett & Glasser, 2009; Hättestrand & Clark, 2006a), and **palaeo-lake shorelines** (erosional or depositional benches parallel

to contours that indicate the presence of glacial lakes; Hättestrand & Clark, 2006a; Bennett & Glasser, 2009).

Meltwater channels – with lengths ranging from ~52 m to ~132 km, with a mean length of ~682 m – occur across the region in a variety of settings, including across lowland terrain, perched on valley sides, and atop morainic ridge crests. To facilitate interpretations of ice sheet dynamics, meltwater channels are classified based on the criteria of Greenwood et al. (2007), as:

*Lateral*: channels formed at the ice margins, observed on slopes oblique to contours.

*Subglacial*: channels reflecting the flow of meltwater beneath an ice sheet, orientated in the direction of ice flow.

*Proglacial*: channels associated with meltwater flowing away from the ice sheet margins.

*Spillway*: channels associated with the drainage of an ice-dammed lake.

Eskers – which range in length from ~41 m to ~49 km, with a mean length of ~1.5 km – represent signatures of subglacial meltwater drainage (Greenwood et al., 2007; Storrar et al., 2014). The eskers are not assigned individual classifications since they are not strictly required for reconstructing former ice sheet dynamics (Kleman & Borgström, 1996). Eskers are predominantly found on the lowland terrain of the western Kola Peninsula and Russian Lapland, and also occur along the White Sea coastline of the eastern Kola Peninsula.

Glaciofluvial deposits are predominantly identified on the western Kola Peninsula and Russian Lapland, as well as along the eastern Kola Peninsula coastline. They occur as large spreads (up to 84 km<sup>2</sup>) on valley floors or terraces perched on valley sides. To support glacial interpretations, glaciofluvial deposits are classified based on the criteria of Bennett et al. (2000), Hättestrand and Clark (2006a), Bennett and Glasser (2009), and Evans and Orton (2015) as:

*Delta*: fan-shaped accumulations of glaciofluvial sediments.

*Terrace*: accumulations of glaciofluvial sediments banked against hillsides, displaying planar upper surfaces and steep fluvial-erosional slopes. Terraces may be ‘stacked’ on hillsides.

*Outwash*: accumulations of glaciofluvial sediments that occur as large spreads (e.g. sandur).

Palaeo-lake shorelines are predominantly identified in the Khibiny Mountains, but can also be found on the lowland terrain in association with morainic deposits. The shorelines are not assigned individual classifications since they are not strictly required for reconstructing former ice sheet dynamics (Kleman & Borgström, 1996).

Lateral meltwater channels are the principal meltwater landform and are found across the mapped area. Lateral meltwater channels indicate: (i) ice margin positions – such as along the southeastern coastline of the peninsula, (ii) ice sheet thinning during deglaciation, when they are identified on plateau summits and on the sides of mountainous areas (Greenwood et al., 2007), and (iii) uninterrupted cold-based glaciation when they are documented in isolation of other glacial landforms – such as on the central eastern Kola Peninsula (Hättestrand & Clark, 2006b; Kleman et al., 2008). In contrast, subglacial meltwater channels and eskers indicate warm-based glaciation in Russian Lapland and along the northern Kola Peninsula coastline (Hättestrand & Clark, 2006b; Kleman et al., 2008). Abundant subglacial meltwater channels are identified on the glacially-scoured bedrock near the northern coast. It is likely that these landforms developed over multiple glacial cycles and/or represent exploited geological faults. Owing to this uncertainty, we have applied a maximum medium confidence (2) to the subglacial meltwater channels near the northern coast, highlighting that they require field checking to assess their glacial origins. Glaciofluvial deposits and palaeo-lake shorelines also signify ice margin positions and are often found in association with meltwater channels and morainic deposits.

### 3.3. Morainic landforms

Morainic landforms include **moraine deposits** (mounds, ridges, or spreads of till and glaciofluvial sediments; Bennett & Glasser, 2009), **moraine ridges** (elongate ridge crests composed of till and glaciofluvial sediments; Bennett & Glasser, 2009), and **cirque infills** (morainic deposits spread across cirque floors and banked against cirque headwalls; Hättestrand et al., 2008).

Moraines are ice-marginal deposits and are mapped here as either **moraine deposits** or **moraine ridges** depending on their morphologies. The spatial distribution of moraines is an important feature necessary for reconstructing ice margin positions, and to aid interpretations of ice dynamics during ice sheet retreat, moraines are classified into the categories outlined in Table 3.

Glacial landforms along the White Sea coastline comprise the most prominent landform assemblage on the eastern Kola Peninsula, which have been documented by previous studies (e.g. Boyes et al., 2021; Hättestrand et al., 2007; Hättestrand & Clark, 2006a; Svendsen et al., 2004). Mapped tabular-shaped interlobate moraines, eskers, meltwater channels, and glaciofluvial deposits suggest that the landform assemblage is ~400 km long: this is ~100 km longer than previous reconstructions propose (cf. Hättestrand et al., 2007; Svendsen et al., 2004). Although



**Table 3.** Moraine classifications applied to the moraine deposit and moraine ridge layers. Diagnostic criteria and examples of moraines on the ArcticDEM imagery are outlined in the Supplementary Data.

Moraine classification	Definition
<i>End</i>	Ridges with defined crests that are aligned perpendicular to ice flow, demarcating the frontal margin of a glacier. End moraine ridges are not used here to demarcate the maximum extent of the ice sheet but represent a significant ice margin.
<i>Lateral</i>	Well-defined ridges are located on mountain sides, above the valley floor, demarcating the lateral margins of a glacier.
<i>De Geer</i>	Ridges aligned perpendicular to ice flow and associated with palaeo-shorelines where the ridges abruptly start/end, demarcating the frontal margins of a glacier in a sub-aqueous environment.
<i>Interlobate</i>	Tabular ridges with steep ice-contact slopes and flat, hummocky, or multi-crested upper surfaces, which form at the edge-to-edge contact of two ice margins.
<i>Hummock – Type 1a</i>	Small irregular mounds and depressions in mountainous environments (e.g. the Khibiny and Lovozero Mountains) associated with Fennoscandian Ice Sheet (FIS) glaciation.
<i>Hummock – Type 1b</i>	Small irregular mounds and depressions associated with localised glaciation (i.e. cirque and icefield glaciations) in mountainous areas.
<i>Hummock – Type 2a</i>	Known as ‘ring-and-ridge moraines’ because of their irregular moraine topography displaying complex ring, ridge, and hummock morphologies. Also known as ‘doughnut’ moraines outside Russia (e.g. Evans et al., 2014). Can occur in large spreads over 600 km <sup>2</sup> .
<i>Hummock – Type 2b</i>	Small irregular mounds and depressions located on the lowland shield terrain associated with FIS glaciation. These moraines can exist as large spreads, up to 400 km <sup>2</sup> .
<i>Hummock – Type 2c</i>	Semi-ordered collections of tabular or ripple-like ridges transverse to ice flow direction. Not to be confused with subglacial ribs.
<i>Hummock – Type 3</i>	Small irregular mounds that may be elongated and/or v-shaped with apices pointed down-ice. Sometimes associated with subglacial drainage (e.g. Lewington et al., 2020; Peterson et al., 2017), but their genetic origins are currently unclear.

its genesis remains uncertain (*cf.* Hättestrand et al., 2007; Svendsen et al., 2004), the significant glaciofluvial landform assemblage mapped here suggests that the landform assemblage is an interlobate formation formed between dynamically different ice masses on the Kola Peninsula and in the White Sea.

Belts of hummocky and end moraines, in places up to 35 km wide, on the lowland shield terrain between the northern and southern coastlines of the western Kola Peninsula indicate multiple palaeo-ice sheet margin positions. This includes a possible Younger Dryas ice-marginal zone, which is determined by comparing the spatial distribution of moraines to other Younger Dryas landforms in Fennoscandia. Hummocky and De Geer moraines in the mountainous areas of the Kola Peninsula and Russian Lapland suggest FIS thinning and ice lobe retreat down-valley during the LGIT. Evidence of localised glaciation is restricted to the Lovozero Mountains, where Type 1b hummocky moraines (Tables 2 and 3) reveal cirque and valley glacier ice margins. This suggests that localised glaciation occurred in the Lovozero Mountains after FIS retreat, although numerical dating controls are required to verify this interpretation.

**Cirque infills** are bouldery deposits located on cirque floors (Hättestrand et al., 2008) with varying surficial morphology in the form of hummocks and ridges. These are included on the map as **cirque infill hummocks** and **cirque infill ridges**. Cirque infills are classified here as *Type 1*, *Type 2*, and *Type 3* according to the morphological criteria of Hättestrand et al. (2008) in order to establish the depositional and post-depositional histories of the deposits. Cirque infill deposits indicate ice sheet thinning in

mountainous areas, possibly under blue ice conditions (Hättestrand et al., 2008; Sugden & Hall, 2020).

### 3.4. Cirques

**Cirques** (amphitheatre-shaped erosional valleys; Evans & Cox, 1995) are located in the mountainous areas of the Kola Peninsula and Russian Lapland, predominantly in the Khibiny and Lovozero Mountains. Cirques are graded according to cirque development following Evans and Cox (1995) and are classified as *simple*, *compound*, *complex*, *staircase*, or *trough* following Benn and Evans (2010). Morainic landforms – including cirque infills and hummocky moraines – located on cirque floors and banked against cirque headwalls indicate ice sheet thinning and retreat down-valley (i.e. away from cirque headwalls) during the LGIT. Cirques, therefore, must have formed before FIS glaciation, later inundated by the FIS during the Late Weichselian.

## 4. Accuracy and completeness

The Kola Peninsula and Russian Lapland was mapped and examined for glacial landforms (digitally and in the field) by a single observer; thus ensuring consistency with regards to bias due to skill and experience in terms of landform identification. Furthermore, field mapping acted to validate the identification and classification criteria used in the construction of this map. The region was systematically examined, and mapping attempted to capture each individual landform. Thus, the map is regarded as an accurate reflection of the spatial distribution of glacial landforms.

Post-glacial modification such as fluvial erosion and anthropogenic influence (the latter of which is minimal in this sparsely populated region) is apparent at the scale of individual landforms. Mapping, therefore, reflects the existing form of the landforms identified in the remotely sensed imagery.

It is estimated that the map is approximately 85% complete; however, the estimated completeness varies for each landform type (Table 1). Smaller and more subtle landforms identified in the taiga forest during field mapping were missed during the digital mapping stage. However, this was not found to be a major issue in the tundra and mountainous locations where tree cover is low. Regardless, such data are not crucial for the purposes of ice sheet-scale reconstructions (Greenwood et al., 2007; Hughes et al., 2010; Kleman & Borgström, 1996). Other landforms were also likely to have been obscured by lakes and reservoirs. The greatest uncertainty is attributed to palaeo-lake shorelines, which may have been reworked by paraglacial processes. Glaciofluvial deposits were also noted to be obscured by vegetation, although to a lesser extent. Thus, it is likely that not all landforms in this region have been identified and included in this map.

## 5. Summary

A total of 245,997 glacial landforms were mapped on the Kola Peninsula and Russian Lapland in northwest Arctic Russia, including a large number of subglacial lineations, meltwater channels, and moraines. The spatial distribution of the mapped landforms shows considerable variation indicative of different basal conditions across the region. For example, while the central eastern Kola Peninsula lacks subglacial bedforms, it is abundant in lateral meltwater channels – both of which indicate cold-based conditions throughout the Late Weichselian (Kleman et al., 2008; Stroeven et al., 2016). In contrast, an abundance of subglacial bedforms in Russian Lapland suggests warm-based conditions during the Late Weichselian (Kleman et al., 2008; Stroeven et al., 2016). Furthermore, zones of densely spaced subglacial lineations probably indicate the presence of palaeo-ice streams (Stokes & Clark, 2001). Additional insight into Late Weichselian glacial conditions in this region may be provided by cirque infill deposits, which may have formed under blue ice conditions (Hättestrand et al., 2008; Sugden & Hall, 2020). Morainic landforms also document ice-marginal positions during deglaciation and may allude to a possible Younger Dryas ice-marginal zone on the peninsula (Hughes et al., 2016; Stroeven et al., 2016).

The map presented here is a new high-resolution regional assessment of glacial landforms and sediments in northwest Arctic Russia. This dataset provides crucial geomorphological data that will be used

(i) in a new glacial reconstruction that aims to reconstruct ice flow patterns at regional- and ice sheet-scales throughout the Late Weichselian, (ii) to reconstruct ice sheet retreat patterns during the LGIT, and (iii) to identify optimal locations for targeted numerical dating of ice-marginal features. This reconstruction will provide an important framework through which numerical ice sheet models can be constrained.

## Data

The data used in the production of this map are provided as supplementary data. The ESRI shapefiles are projected using the WGS84 datum. The classifications and confidence ratings for each feature can be viewed in the attribute table of the shapefiles.

## Software

Relief shaded visualisations of the ArcticDEM dataset, provided by the Polar Geospatial Center under NSF-OPP awards 1043681, 1559691, and 1542736 (Porter et al., 2018), were produced using *ESRI® ArcMap™ 10.7.1* (herein ArcMap). PlanetScope Ortho Scene data, courtesy of Planet, were combined into a single seamless image in ArcMap. *Google Earth Pro* was used for 3D landform visualisation and virtual reconnaissance. On-screen digitisation of landform crest-line or break-of-slope was conducted in ArcMap. The map was produced in ArcMap, and imported into *Adobe Illustrator v24.2* where final layout work was completed prior to exporting as a PDF.

## Acknowledgements

We particularly thank Yulia Zaika (INTERACT), Andrey Vashkov, and the late Professor Vasili Kolka, all at the Kola Science Centre of the Russian Academy of Sciences in Apatity, who provided scientific and logistic assistance for fieldwork. Chris Orton, Chris Clark, Isabelle McMartin, and Ola Fredin are gratefully acknowledged for providing useful comments on both the map and manuscript.

## Disclosure statement

No potential conflict of interest was reported by the author(s).

## Funding

This work was undertaken while BMB was in receipt of a University of Brighton PhD Studentship. Fieldwork was supported by two INTERACT funded projects [grant numbers 262693 and 730938].

## References

Barr, I. D., & Spagnolo, M. (2015). Glacial cirques as palaeoenvironmental indicators: Their potential and

- limitations. *Earth-Science Reviews*, 151, 48–78. <https://doi.org/10.1016/j.earscirev.2015.10.004>
- Benn, D. I., & Evans, D. J. A. (2010). *Glaciers and glaciation*. Hodder Education.
- Bennett, M. R., & Glasser, N. F. (2009). *Glacial geology: Ice sheets and landforms*. John Wiley & Sons.
- Bennett, M. R., Huddart, D., & McCormick, T. (2000). The glaciolacustrine landform-sediment assemblage at Heinabergsjökull, Iceland. *Geografiska Annaler: Series A, Physical Geography*, 82(1), 1–16. <https://doi.org/10.1111/j.0435-3676.2000.00107.x>
- Boyes, B. M., Linch, L. D., Pearce, D. M., Kolka, V. V., & Nash, D. J. (2021). The Kola Peninsula and Russian Lapland: A review of Late Weichselian glaciation. *Quaternary Science Reviews*, 267, 107087. <https://doi.org/10.1016/j.quascirev.2021.107087>
- Chandler, B. M. P., Lovell, H., Boston, C. M., Lukas, S., Barr, I. D., Benediktsson, Í. Ó., Benn, D. I., Clark, C. D., Darvill, C. M., Evans, D. J. A., Ewertowski, M. W., Loibl, D., Margold, M., Otto, J. C., Roberts, D. H., Stokes, C. R., Storrar, R. D., & Stroeven, A. P. (2018). Glacial geomorphological mapping: A review of approaches and frameworks for best practice. *Earth-Science Reviews*, 185, 806–846. <https://doi.org/10.1016/j.earscirev.2018.07.015>
- Chiverrell, R. C., Thomas, G. S. P., Burke, M., Medialdea, A., Smedley, R., Bateman, M. D., Clark, C. D., Duller, G. A. T., Fabel, D., Jenkins, G., Ou, X. J., Roberts, H. M., & Scourse, J. (2020). The evolution of the terrestrial-terminating Irish Sea glacier during the last glaciation. *Journal of Quaternary Science*, 28. <https://doi.org/10.1002/jqs.3229>
- Clark, C. D., Ely, J. C., Greenwood, S. L., Hughes, A. L. C., Meehan, R., Barr, I. D., Bateman, M. D., Bradwell, T., Doole, J., Evans, D. J. A., Jordan, C. J., Monteys, X., Pellicer, X. M., & Sheehy, M. (2018). BRITICE glacial map, version 2: A map and GIS database of glacial landforms of the last British-Irish Ice Sheet. *Boreas*, 47(1), 11–27. <https://doi.org/10.1111/bor.12273>
- Ekman, I., & Iljin, V. (1991). *Deglaciation, the Younger Dryas end moraines and their correlation in the Karelian A.S.S.R and adjacent areas*. Geological Survey of Finland.
- European Space Agency, Sinergise. (2021). *Copernicus global digital elevation model*. OpenTopography.
- Evans, D. J. A., & Orton, C. (2015). Heinabergsjökull and Skalafellsjökull, Iceland: Active temperate piedmont lobe and outwash head glacial landsystem. *Journal of Maps*, 11(3), 415–431. <https://doi.org/10.1080/17445647.2014.919617>
- Evans, D. J. A., Young, N. J. P., & Ó Cofaigh, C. (2014). Glacial geomorphology of terrestrial-terminating fast flow lobes/ice stream margins in the southwest Laurentide Ice Sheet. *Geomorphology*, 204, 86–113. <https://doi.org/10.1016/j.geomorph.2013.07.031>
- Evans, I. S., & Cox, N. J. (1995). The form of glacial cirques in the English Lake District, Cumbria. *Zeitschrift Fur Geomorphologie*, 39(2), 175–202. <https://doi.org/10.1127/zfg/39/1995/175>
- GEBCO Compilation Group. (2020). GEBCO 2020 Grid.
- Greenwood, S. L., & Clark, C. D. (2008). Subglacial bedforms of the Irish Ice Sheet. *Journal of Maps*, 4(1), 332–357. <https://doi.org/10.4113/jom.2008.1030>
- Greenwood, S. L., Clark, C. D., & Hughes, A. L. C. (2007). Formalising an inversion methodology for reconstructing ice-sheet retreat patterns from meltwater channels: Application to the British Ice Sheet. *Journal of Quaternary Science*, 22(6), 637–645. <https://doi.org/10.1002/jqs.1083>
- Grosswald, M. G., & Hughes, T. J. (2002). The Russian component of an Arctic Ice Sheet during the last glacial maximum. *Quaternary Science Reviews*, 21(1–3), 121–146. [https://doi.org/10.1016/S0277-3791\(01\)00078-6](https://doi.org/10.1016/S0277-3791(01)00078-6)
- Hättestrand, C., & Clark, C. D. (2006a). The glacial geomorphology of Kola Peninsula and adjacent areas in Murmansk Region, Russia. *Journal of Maps*, 30–42. <https://doi.org/10.4113/jom.2006.41>
- Hättestrand, C., & Clark, C. D. (2006b). Reconstructing the pattern and style of deglaciation of Kola Peninsula, north-eastern Fennoscandian Ice Sheet. In P. G. Knight (Ed.), *Glacier science and environmental change*. Blackwell Publishing. <https://doi.org/10.1002/9780470750636.ch39>
- Hättestrand, C., Kolka, V. V., & Johansen, N. (2008). Cirque infills in the Khibiny Mountains, Kola Peninsula, Russia – palaeoglaciological interpretations and modern analogues in East Antarctica. *Journal of Quaternary Science*, 23(2), 165–174. <https://doi.org/10.1002/jqs.1130>
- Hättestrand, C., Kolka, V. V., & Stroeven, A. P. (2007). The Keiva ice marginal zone on the Kola Peninsula, northwest Russia: A key component for reconstructing the palaeoglaciology of the northeastern Fennoscandian Ice Sheet. *Boreas*, 36(4), 352–370. <https://doi.org/10.1080/03009480701317488>
- Hughes, A. L. C., Clark, C. D., & Jordan, C. J. (2010). Subglacial bedforms of the last British Ice Sheet. *Journal of Maps*, 6(1), 543–563. <https://doi.org/10.4113/jom.2010.1111>
- Hughes, A. L. C., Gyllencreutz, R., Lohne, O. S., Mangerud, J., & Svendsen, J. I. (2016). The last Eurasian ice sheets – a chronological database and time-slice reconstruction, DATED-1. *Boreas*, 45(1), 1–45. <https://doi.org/10.1111/bor.12142>
- Kleman, J., & Borgström, I. (1996). Reconstruction of palaeo-ice sheets: The use of geomorphological data. *Earth Surface Processes and Landforms*, 21(10), 893–909. [https://doi.org/10.1002/\(SICI\)1096-9837\(199610\)21:10<893::AID-ESP620>3.0.CO;2-U](https://doi.org/10.1002/(SICI)1096-9837(199610)21:10<893::AID-ESP620>3.0.CO;2-U)
- Kleman, J., Hättestrand, C., Borgström, I., & Stroeven, A. P. (1997). Fennoscandian palaeoglaciology reconstructed using a glacial geological inversion model. *Journal of Glaciology*, 43(144), 283–299. <https://doi.org/10.1017/S0022143000003233>
- Kleman, J., Stroeven, A. P., & Lundqvist, J. (2008). Patterns of quaternary ice sheet erosion and deposition in Fennoscandia and a theoretical framework for explanation. *Geomorphology*, 97(1–2), 73–90. <https://doi.org/10.1016/j.geomorph.2007.02.049>
- Lavrova, M. A. (1960). *Quaternary geology of the Kola Peninsula*. Academia Science Press (in Russian).
- Lewington, E. L. M., Livingstone, S. J., Clark, C. D., Sole, A. J., & Storrar, R. D. (2020). A model for interaction between conduits and surrounding hydraulically connected distributed drainage based on geomorphological evidence from Keewatin, Canada. *Cryosphere*, 14(9), 2949–2976. <https://doi.org/10.5194/tc-14-2949-2020>
- McMartin, I., Godbout, P.-M., Campbell, J. E., Tremblay, T., & Behnia, P. (2021). A new map of glacial features and glacial land systems in central mainland Nunavut, Canada. *Boreas*, 50(1), 51–75. <https://doi.org/10.1111/bor.12479>
- Niemelä, J., Ekman, I., & Lukashov, A. (1993). *Quaternary deposits of Finland and northwestern part of Russian Federation and their resources: Map at 1: 1,000,000*. Geological Survey of Finland and Institute of Geology, Karelian Science Centre of the Russian Academy of Sciences.

- Ojala, A. E. K., Mäkinen, J., Ahokangas, E., Kajuutti, K., Valkama, M., Tuunainen, A., & Palmu, J.-P. (2021). Diversity of murtoos and murtoo-related subglacial landforms in the Finnish area of the Fennoscandian Ice Sheet. *Boreas*. <https://doi.org/10.1111/bor.12526>
- Peterson, G., Johnson, M. D., & Smith, C. A. (2017). Glacial geomorphology of the south Swedish uplands – focus on the spatial distribution of hummock tracts. *Journal of Maps*, 13(2), 534–544. <https://doi.org/10.1080/17445647.2017.1336121>
- Porter, C., Morin, P., Howat, I., Noh, M.-J., Bates, B., Peterman, K., Keesey, S., Schlenk, M., Gardiner, J., Tomko, K., Willis, M., Kelleher, C., Cloutier, M., Husby, E., Foga, S., Nakamura, H., Platson, M., Wethington, M., Williamson, C., ... Bojesen, M. (2018). *ArcticDEM*. Harvard Dataverse, V1 ed.
- Rainio, H., Saarnisto, M., & Ekman, I. (1995). Younger Dryas end moraines in Finland and NW Russia. *Quaternary International*, 28, 179–192. [https://doi.org/10.1016/1040-6182\(95\)00051-J](https://doi.org/10.1016/1040-6182(95)00051-J)
- Smith, M. J., & Clark, C. D. (2005). Methods for the visualization of digital elevation models for landform mapping. *Earth Surface Processes and Landforms*, 30(7), 885–900. <https://doi.org/10.1002/esp.1210>
- Smith, M. J., Rose, J., & Booth, S. (2006). Geomorphological mapping of glacial landforms from remotely sensed data: An evaluation of the principal data sources and an assessment of their quality. *Geomorphology*, 76(1–2), 148–165. <https://doi.org/10.1016/j.geomorph.2005.11.001>
- Stokes, C. R., & Clark, C. D. (2001). Palaeo-ice streams. *Quaternary Science Reviews*, 20(13), 1437–1457. [https://doi.org/10.1016/S0277-3791\(01\)00003-8](https://doi.org/10.1016/S0277-3791(01)00003-8)
- Stokes, C. R., Margold, M., & Creyts, T. T. (2016). Ribbed bedforms on palaeo-ice stream beds resemble regular patterns of basal shear stress ('traction ribs') inferred from modern ice streams. *Journal of Glaciology*, 62(234), 696–713. <https://doi.org/10.1017/jog.2016.63>
- Stokes, C. R., Tarasov, L., Blomdin, R., Cronin, T. M., Fisher, T. G., Gyllencreutz, R., Hättestrand, C., Heyman, J., Hindmarsh, R. C. A., Hughes, A. L. C., Jakobsson, M., Kirchner, N., Livingstone, S. J., Margold, M., Murton, J. B., Riko, N., Peltier, W. R., Peteet, D. M., Piper, D. J. W., ... Teller, J. T. (2015). On the reconstruction of palaeo-ice sheets: Recent advances and future challenges. *Quaternary Science Reviews*, 125, 15–49. <https://doi.org/10.1016/j.quascirev.2015.07.016>
- Storrar, R. D., Stokes, C. R., & Evans, D. J. A. (2014). Morphometry and pattern of a large sample (>20,000) of Canadian eskers and implications for subglacial drainage beneath ice sheets. *Quaternary Science Reviews*, 105, 1–25. <https://doi.org/10.1016/j.quascirev.2014.09.013>
- Stroeven, A. P., Hättestrand, C., Kleman, J., Heyman, J., Fabel, D., Fredin, O., Goodfellow, B. W., Harbor, J. M., Jansen, J. D., Olsen, L., Caffee, M. W., Fink, D., Lundqvist, J., Rosqvist, G. C., Strömberg, B., & Jansson, K. N. (2016). Deglaciation of Fennoscandia. *Quaternary Science Reviews*, 147, 91–121. <https://doi.org/10.1016/j.quascirev.2015.09.016>
- Sugden, D., & Hall, A. M. (2020). Antarctic blue-ice moraines: Analogue for Northern Hemisphere ice sheets? *Quaternary Science Reviews*, 249. <https://doi.org/10.1016/j.quascirev.2020.106620>
- Svendsen, J. I., Alexanderson, H., Astakhov, V. I., Demidov, I. N., Dowdeswell, J. A., Funder, S., Gataullin, V., Henriksen, M., Hjort, C., Houmark-Nielsen, M., Hubberten, H. W., Ingólfsson, Ó, Jakobsson, M., Kjær, K. H., Larsen, E., Lokrantz, H., Lunkka, J. P., Lyså, A., Mangerud, J., ... Stein, R. (2004). Late quaternary ice sheet history of northern Eurasia. *Quaternary Science Reviews*, 23(11–13), 1229–1271. <https://doi.org/10.1016/j.quascirev.2003.12.008>
- Winsborrow, M. C. M., Andreassen, K., Corner, G. D., & Laberg, J. S. (2010). Deglaciation of a marine-based ice sheet: Late Weichselian palaeo-ice dynamics and retreat in the southern Barents Sea reconstructed from onshore and offshore glacial geomorphology. *Quaternary Science Reviews*, 29(3–4), 424–442. <https://doi.org/10.1016/j.quascirev.2009.10.001>
- Yevzerov, V. Ye. (2015). The structure and formation of the outer strip of one of the marginal belts of the Late Valdaian ice sheet in the Kola region. *Vestnik VSU. Series: Geology*, 4, 5–12 (in Russian).